Self-Assembling Peptide-Appended Metallomacrocycle Pores for Selective Water Translocation

Li-Bo Huang, Fumihiko Mamiya, Marc Baaden, Eiji Yashima, Mihail Barboiu

Self-Assembling Peptide-Appended Metallomacrocycle Pores for Selective Water Translocation

Li-Bo Huang, [#,⍰] Fumihiko Mamiya, [†] Marc Baaden,[¶] Eiji Yashima, [†,ψ*] and Mihail Barboiu[#,*]

[#]Institut Europeen des Membranes, Adaptive Supramolecular Nanosystems Group, University of Montpellier, ENSCM-CNRS, UMR5635, Place E. Bataillon CC047, 34095 Montpellier, France

[†]Department of Molecular Design and Engineering, Graduate School of Engineering, Nagoya University Chikusa-ku, Nagoya 464-8603, Japan

[¶]Laboratoire de Biochimie Théorique, CNRS, Université Paris Cité, 13 rue Pierre et Marie Curie, F-75005, Paris, France

[ψ] Department of Molecular and Macromolecular Chemistry, Graduate School of Engineering, Nagoya University Chikusa-ku, Nagoya 464-8603, Japan

[⍰]School of Chemical Engineering and Technology, Hainan University, Haikou 570228, China

KEYWORDS: artificial water channels, porins, self-assembly, water clusters, macrocycles

ABSTRACT: Artificial water channels-AWCs selectively transport water, excluding all ions. Unimolecular channels been synthesized *via* complex synthetic steps. Ideally, simpler compounds requesting less synthetic steps should efficiently lead to selective channels by self-assembly. Herein, we report a self-assembled peptide-bound Ni^{2+}-metallomacrocycle, **1**, in which rim-peptide-bound units are connected to a central macrocycle obtained via condensation in the presence of Ni^{2+} ions. Compound **1** achieves a single-channel permeability up to 10^7-10^8 water/s/channel and insignificant ion transport, which is one order of magnitude lower as for Aquaporins. Molecular simulations probe that sponge-like aggregates can form to generate transient cluster water pathways through the bilayer. Altogether, the adaptive metallo-supramolecular self-assembly is an efficient and simple way to construct selective channel superstructures.

INTRODUCTION

The selective transport of metabolites across bilayer membranes in living cells is facilitated by simple molecular carriers or by complex protein channels.[1–3] Biomimetic artificial channels have been designed to understand the translocation mechanisms of ions and water molecules through the membranes and used as active components of sensing, separation and delivery devices.[4] Single molecule spanning the bilayer membranes, have been used in an early stage by the researchers pioneering the field, to construct synthetic channels.[5–8] They are positioned as a macrocyclic scaffolding relay in the middle of the membrane, whereas functional groups attached to this central relay form bundles, closing a unimolecular pillared channel. Significant progress has recently been obtained in this field, when Hou et al. realized that pillar[x]arenes x = 4,5 – PA can be used as a scaffolding relay,[9-11] whereas functional groups attached to aromatic rings form unimolecular pillared channels, replacing natural aquaporins in cells.[12] We recently described that dimerization of rim-differentiated PAs, produces expanded channels with osmotic water permeability close to natural aquaporins.[13,14]

Another attractive strategy for the construction of biomimetic channels is based on the self-assembly of several building blocks towards the creation of supramolecular channels.[15] Most of the reported channels are composed of organic molecules self-assembled *via* H-bonds.[16,17] Metallo-supramolecular architectures, presenting ionic conductance states in bilayer membranes have been reported during the last decade.[15] Fyles et al.[18] was pioneering the field and incipiently demonstrated that large supramolecular channels with internal pore diameters of 10 nm can be assembled from organic building blocks and metal cations.

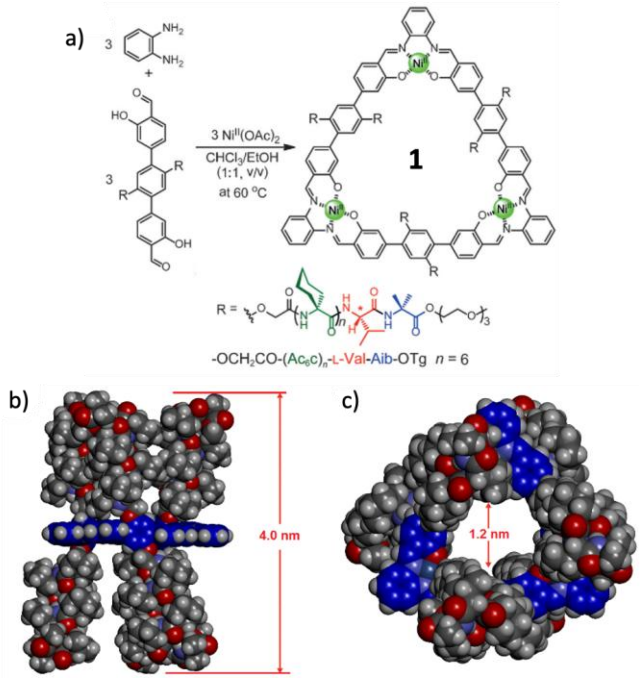

Figure 1. (a) Chemical formula and (b) lateral and (c) top views of the energy minimized structures of pep-tide-bound Ni2+-salphen-based metallomacrocycle, **1**.

They started to construct such scaffolds based on a lipophilic Fujita's square complex,[19] but it was shown that the lipophilic pore is more complex and is composed of several Pd^{2+} centers in the bilayer membrane. This was the starting point to explore other functional channels based on metal-organic complex polyhedra.[20-23] This simple and effective strategy may conveniently demonstrate the potential of using simple molecules and metal ions to easily generate biomimetic nanopores with ion channel activity in lipid bilayers, avoiding complex synthetic steps required by the design of single-molecular channel.

EXPERIMENTAL SECTION

Transmembrane transport experiments

Sample preparation. We set the concentration gradients (15, 20, 25, 30 μM) of complex 1 solution in DMSO for water transport assays. When injected into large unilamellar vesicles (LUV) suspension, the final concentration of complex 1 became 0.15, 0.2, 0.25 and 0.3 μM, corresponding to the molar channel to lipid ratio (mCLR) = 0.034, 0.046, 0.058 and 0.070 mol%. In the cation transport HPTS (pyranine, 8-hydroxypyrene-1,3,6-trisulfonic acid trisodium salt) assays, we added complex 1 by premixing method when preparing LUV, and the final concentrations of complex 1 in LUV suspension were 0.14, 0.17, 0.22, 0.25 and 0.28 μM, corresponding to mCLR = 0.025, 0.030, 0.040, 0.045 and 0.050 mol%. It is noteworthy that the composition of LUV used in water transport assays and cation transport assays was different.

Water transport by using D(+)-sucrose as osmolyte. LUV were prepared using the film rehydration method. A phosphatidylcholine, phosphatidylserine and cholesterol PC/PS/Chl mixture with a molar ratio of 4/1/5 was dissolved in chloroform/methanol mixture ($CHCl_3$/MeOH, v/v: 1/1). The solution was dried on a rotary evaporator and subsequently in a vacuum desiccator to remove residual solvent. After rehydration with 1 mL buffer containing 200 mM sucrose and 10 mM PBS (pH = 6.4), the suspension was extruded through 100 nm track-etched filters for 21 times (Whatman, UK) to obtain monodisperse unilamellar vesicles, the size of which was characterized by dynamic light scattering (Zetasizer Nano, Malvern Instruments Ltd., UK). The aliquots of complex **1** dissolved in DMSO have been added to the LUV. The water permeability tests were conducted on a stopped-flow instrument (SFM3000 + MOS450, Bio-Logic SAS, Claix, France). Exposure of vesicles to hypertonic osmolyte (300 mM sucrose) in the same buffer resulted in the shrinkage of the vesicles due to an outwardly directed osmotic gradient. The changes of light scattering were recorded at a wavelength of 345 nm. The abrupt change of the vesicle size led to variation in the light scattering at 90° according to the Rayleigh-Gans theory applied to this system and could be fitted in the form of the sum of double-exponential functions.

The osmotic permeability (Pf) was calculated as following:

$$P_f = \frac{\mathrm{k}}{\frac{S}{V_0} \times V_w \times \Delta_{osm}}$$

where k is the smaller exponential coefficient (k_1) obtained by fitting the light scattering traces into double-exponential functions, because the larger exponential coefficient (k_2) showed no apparent functional relationship with increasing permeability in these assays; S and V_0 are the initial surface area and volume of the vesicles, respectively; V_w is the molar volume of water, and Δ_{osm} is the osmolarity difference.

In an average experiment, 100 μL stock lipid solution containing 0.524 mg of lipids was diluted with 1880 μL of 200 mM sucrose or 115 mM NaCl in 10 mM PBS buffer solution. The complex 1 were injected in 20 μL aliquots in DMSO. The solution mix was maintained at 20 ℃ for 30 minutes before exposure to the 400 mM sucrose solution. Experiments have been conducted at different concentrations of the injected complex **1**, in which the mCLR of complex 1 in LUV suspension were 0.034, 0.046, 0.058 and 0.070 mol%. Average permeability was calculated by using the permeability values obtained from at least three different batches of vesicles.

Single-channel permeability calculations. One complex is needed to form a channel within a transmembrane length of 5 nm. Taking the sample at 0.20 μM as an example, the molar channel to lipid ratio is 0.046 mol%. The average radius of the liposome was 72.5 nm determined by DLS experiments. Hence, the sum of outer and inner surface areas was $4\pi \times R^2 + 4\pi \times (R - 5)^2 = 123{,}308$ nm^2. The average cross-sectional area of a lipid in average was 0.287 nm (PC/PS/Chl lipids with a molar ratio of 4/1/5: the cross-sectional areas of PC and PS were ~0.35 nm^2 and that of cholesterol was 0.223 nm^2), and that of the channel was estimated as 2.80 nm^2. So, the insertion number of the channel was ~98 per vesicle. If the overall net permeability by channels in liposomes was (3.05 ± 0.47) μm/s, the single-channel permeability was (1.91 ± 0.29) × 10^{-15} cm^3/s and (6.38 ± 0.98) × 10^7 water molecules/s. According to the same algorithm, the single-channel permeabilities for the channels at different mCLR were shown in Table S1 and S2. The single-channel permeability values covered the range of 1.8 × 10^7–6.4 × 10^7 H2O/s/channel, which are within the same order of magnitude as that of Aquaporins (~10^8–10^9 water molecules/s/channel).

Water transport by using NaCl as osmolyte. The preparation of liposomes and the stopped-flow assays were the same as the previous method for water transport in sucrose solution. To implement the same osmotic pressure (106 mOsmol/kg), the concentration of NaCl osmolyte was different from D(+)-sucrose. Internal: 115 mM NaCl and 10 mM PBS, pH = 6.4; External: 172.5 mM NaCl and 10 mM PBS, pH = 6.4 (after mixture).

Cation transport HPTS assays.

LUV preparation. The complex 1 and egg yolk L-α-phosphatidylcholine (EYPC chloroform solution, 800 μL, 26 mmol) were dissolved in a $CHCl_3$/MeOH mixture, the solution was evaporated under reduced pressure and the resulting thin film was dried in a vacuum desiccator for 2 h. The lipid film was hydrated in 400 μL phosphate buffer (10 mM sodium phosphate, pH = 6.4, 100 mM NaCl) containing 10 μM HPTS for 40 min. During hydration, the suspension was submitted to at least 7 freeze-thaw cycles (bathed in liquid nitrogen and water at room temperature, respectively). The large multilamellar liposome suspension

(1 mL) was submitted to high-pressure extrusion at room temperature (21 extrusions through a 100 nm polycarbonate membrane afforded a suspension of LUVs with an average diameter of ~100 nm). The LUV suspension was separated from extravesicular dye by size exclusion chromatography (SEC) (stationary phase: Sephadex G-50, mobile phase: phosphate buffer) and diluted to 2.8 mL with the same PBS buffer to give a stock solution with a lipid concentration of 9.3 mM (assuming 100% of lipid was incorporated into liposomes).

Cation transport. 100 µL HPTS-loaded vesicles (stock solution) was suspended in 1.86 mL sodium phosphate, pH = 6.4 with 100 mM MCl (M = Na^+, K^+, Rb^+ or Cs^+) and placed into a quartz fluorimetric cuvette. The emission of HPTS at 510 nm was monitored with excitation wavelengths at 403 and 460 nm simultaneously, using a Perkin Elmer LS-55 fluorescence spectrometer. During the experiment, 29 µL of 0.5 M aqueous NaOH was injected at t = 20 s, resulting in the pH value increasing to around 7 in the extravesicular media. For the reference proton transport experiment, 20 µL of 50 µM carbonyl cyanide-4-(trifluoromethoxy)phenylhydrazone (FCCP) solution in DMSO was added at t = 10 s. Maximal possible changes in dye emission were obtained at t = 320 s by lysis of the liposomes with detergent (40 µL of 5 % aqueous Triton X100). We expressed normalized intensity (the value of I_{460}/I_{405}) as a function of time from t = 0 s to 320 s. To calculate EC_{50} and Hill coefficient n, we used the fractional activity Y. Y was calculated for each curve using the normalised value of I_{460}/I_{403} (just before lysis of the vesicles), from 0 (ratio for the blank) to 1 (highest ratio obtained, i.e. a plateau). We expressed Y as a function of time, and we performed fittings using a 2-parameter equation, which is, Hill equation:

$$Y = \frac{1}{1 + (EC_{50}/[C])^n}$$

The Hill coefficient is an indication the cooperativity of the channel forming elements. There is two ways to find Hill coefficient n and EC_{50}: either fitting of the experimental curve using the Hill function (as we did), or using the expression:

$$log\left(\frac{Y}{1-Y}\right) = nlogC - nlogEC_{50}$$

where n is the slope of the curve and n*log (EC_{50}) is the log(C) = 0 intercept value.

Molecular dynamics simulations of compound 1 channels in a fully hydrated lipid bilayer environment.

To prepare the starting point used for the simulations, the macrocycle had to be subdivided into smaller "residues", 3 identical ones for the cycle itself, 6 for the core of the branched R chains and 6 for the terminal OTG groups as illustrated in Figure 3a. We also set up a 7-mer aggregate in the membrane as simulation C1-NI2-x7, using our own virtual reality tools to assemble a tight initial complex from a pre-equilibrated monomer along the protocol described,28 which was run for 105 ns. During the equilibration of the simulations we manually wetted the channel interior to stabilize the hollow structure, and attempted to fix atom positions of the macrocycle and the included waters in the beginning of the equilibration period.

The C1-NI2 simulation was set up automatically by aligning the macrocycle axis with the membrane normal, which was then oriented along the Y-axis, normally with respect to the plane of the membrane and the XZ-plane. Having placed an equilibrated membrane structure (consisting of phosphatidyl-choline molecules) at this location named 'MemCenterY', the system was enclosed in a simulation cell of size 65*63*65 Å, the macrocycle was temporarily scaled by 0.9 along the XZ-axes, then strongly clashing membrane lipids were deleted (lipids with an atom closer than 0.75 Å to a macrocycle atom). The temporary macrocycle scaling, which was needed to avoid the deletion of too many lipids around the protein, was then slowly removed during a short simulation at 298K in vacuo: the macrocycle (with all atoms kept fixed) was scaled by 1.02 along the XZ-axes every 200 femtoseconds, while the membrane was allowed to move, but restrained to ideal geometry (by pulling lipid residues with an atom further than 21.5 Å away from MemCenterY back into the membrane, and by pushing phosphorus atoms closer than 14 Å to MemCenterY back outwards). The force field was AMBER14, with Lipid14/GAFF/AM1BCC parameters for non-standard residues. As soon as the macrocycle had reached its original size again, the simulation cell was filled with water, 0.9% NaCl and counter ions The main simulation was then run with PME and 8.0 Å cutoff for non-bonded real space forces, a 4 fs time-step, constrained hydrogen atoms, and at constant pressure and temperature (NPT ensemble), as described in detail previously. During the initial 250 picoseconds, the membrane was restrained to avoid distortions while the simulation cell adapted to the pressure exerted by the membrane (see above, additionally water molecules that got closer than 14 Å to MemCenterY were pushed outside). The source code of this simulation protocol and visualizations of the individual steps can be found at www.yasara.org/membranemd. C1-NI2-x7 was set up in a similar way, with a larger initial cell size.

RESULTS AND DISCUSSION

Design strategy. Herein we concentrate our efforts on investigation of water/ion transport properties through lipid bilayer membranes containing self-assembled discrete peptide-bound Ni^{2+}-salphen-based metallomacrocycle, **1** (Figure 1), in which rim-peptide-bound phenylene units are connected to a central metallomacrocycle. Tubular channel superstructures are obtained through self-assembly *via* multiple imine/coordination reactions of the peptide-bound disalicylaldehyde with ortho-phenylenediamine in the presence of Ni^{2+} acetate. The synthesis previously reported by Yashima et al. is quantitatively leading to the trimeric macrocycle in high yields (92–97%).[24] The unprecedented dynamic planar chirality observed with compound **1** is crucial for maintaining the pR/pS interconversion in this system while it might be strongly suppressed when the compounds is embedded in a bilayer membrane environment.

The hydrophobic nature of the peptide arms may provide not only an important solubility of these compounds in the membrane, but more important a rational design

strategy for developing macrocycle-based ion channels that make use of 3_{10}-to-a-helix transitions to regulate the opening of the pores and implicitly the selectivity of the transport.[24] Other hydrophobic peptides scaffolded around synthetic pillarene[9-12] or cyclodextrins[25] have been developed and inserted into bilayers.

Interestingly, the analysis of an energy minimized structure of **1** shows the formation of a dynamic bundle-type unimolecular channel architecture. This scaffold might allow the translocation of partly dehydrated cations or water molecules along well-fitting membrane inserted channels of 4.0 nm theoretical length (Figure 1b), formed *via* self-assembled double-faced lateral peptide arms anchored to a large central pore of 1.2 nm diameter (Figure 1c). We anticipated that closely spaced peptide appended metallomacrocycle **1** would allow interactional translocation, restriction and control of the transport activity within a central selectivity filter, as for natural proteins.

Water-Transport Experiments. The peptide-bound Ni^{2+}-salphen-based macrocycle channels, **1**, were reconstituted into lipid vesicles (100 nm in diameter) of phosphatidylcholine/phosphatidylserine/cholesterol (PC/PS/ Chl, 4/1/5, molar ratio) containing 200 mM D-(+)-sucrose or 115 mM NaCl in 10 mM PBS, buffer solution (pH = 6.4). The complex **1** was added from their DMSO solutions to pre-formed vesicles. Then, the vesicles were exposed to outwardly hypertonic conditions driven by 10 mM PBS buffer solution (pH = 6.4) of 300 mM D-(+)-sucrose or 172.5 mM NaCl osmolytes, to evidence the shrinkage of the liposomes that increased the light-scattering signal (Figure 2a,b).

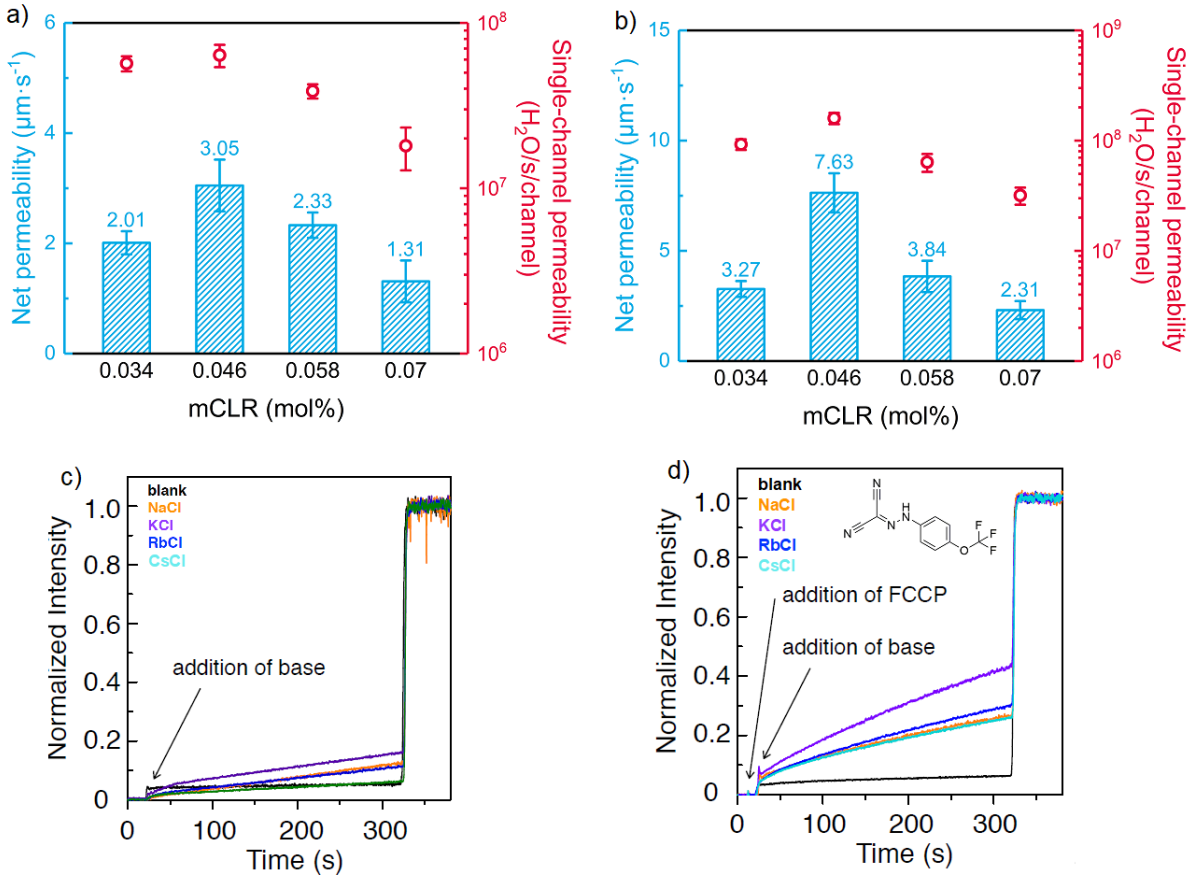

Figure 2. Water net permeability and single-channel permeability values determined at different concentrations of channels in the liposomes by using stopped-flow light scattering experiments and (a) D-(+)-sucrose or (b) NaCl as osmolytes. Comparison of M^+ = Na^+, K^+, Rb^+ and Cs^+ transport activities expressed as normalized fluorescence intensity of 0.14 μM (0.025 mol%) channels in the extravesicular media containing 100 mM MCl, (c) in the absence or (d) with the presence of FCCP as H^+ carrier. Maximal possible dye emission is obtained at t = 320 s by lysis of the liposomes with detergent Triton X100.

Unfortunately the experimental water transport rates are not very high, however interesting improvements for initial rates were observed when the water channels are added in the membrane. If such water transport rates are very close, then a first order fitting method will give you an accurate value of an improved water rate. The k value for water transport can be then obtained by subtracting the control rate. The water transport rates are strongly dependent on the molar channel to lipid ratio (mCLR) of **1**: 0.034, 0.046, 0.058, 0.070 mol%, that increase the net water permeability relative to the background lipid permeability in the bilayer membrane (Figures 2a). It can be noticed that with 100 mM D-(+)-sucrose osmolarity (Δosm = 106 mOsmol / kg) the net channel permeabilities remain on the same level of magnitude ~2 μm/s for all concentrations (Figure 2a). The single channel permeability values

covered the range of 1.8×10^7–6.4×10^7 H2O/s/channel and they are decreasing with increasing concentration. The net channel permeabilities are improved and show a tendency of increasing up to ~7.62 μm/s with 57.5 mM NaCl osmolarity (Δosm = 106 mOsmol/kg) (Figure 2b). The increasing permeabilities values in the presence of metallomacrocycle, **1** are interesting, however they are not out competing the natural water translocating counterparts.

Cation and Proton-Transport Experiments Cation (M^+ = Na^+, K^+, Rb^+ and Cs^+) transport activities across the bilayer membranes incorporating channels **1**, reconstituted into phosphatidylcholine (PC) lipid vesicles (100 nm), were assessed using standard HPTS fluorescence assays (Figure 2c,d, S1-S5).[27,28] Indeed, when tested with MCl on external buffer, the channel **1** does not present a dose-response-type activity, showing very low (< 10%) or near to zero activity behaviors (Figure 2c), reminiscent with negligeable M^+/H^+ antiport conductance states of the channels **1** in the membrane. This confirms our initial assumption a restricted transport of the hydrated cations may occur through the hydrophobic sterically restricted pore formed by the peptide arms. In order to verify if the H^+ transport is the rate-limiting step for M^+/H^+ antiport activity, we conducted HPTS assays with compounds **1** in the presence of carbonyl cyanide-4-(trifluoromethoxy)-phenylhydrazone, FCCP as a H^+ carrier (Figure 2d, S1-S7).[28] These experiments have shown a difference with the previous results suggesting increased cation transport activities for all MCl salts in the presence of 0.14 to 0.28 μM of **1**. Among them, the lowest value of $EC_{50(K^+)}$ = 17.4 μM is observed for K^+ (Table S3). However the transport selectivity for K^+ is very low when compared with other cations : $EC_{50(Na^+)}$ = 20.9 μM, $EC_{50(Rb^+)}$ = 19.5 μM, $EC_{50(Cs^+)}$ = 20.9 μM. Hill coefficients are for all the cations from 1.5 to 2 and are indicative of a high degree of cooperativity for cation transport. On this basis, the resulting rather weak transport selectivity, indicates that the transport of the hydrated anions is slightly governed by the solvation free energy of the cations and most probably related to a competitive Cl^-/H^+ symport.

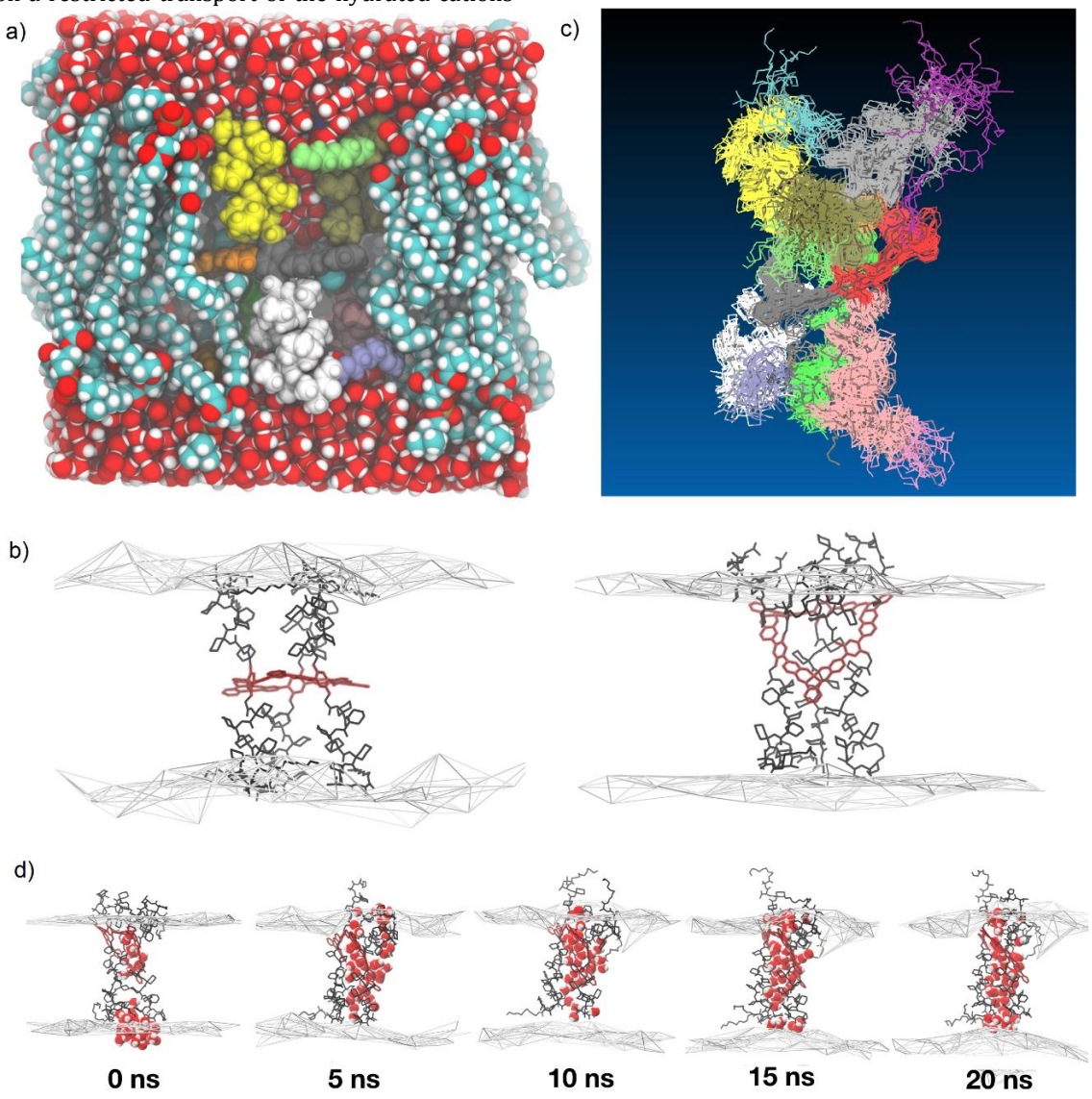

Figure 3. (a) Schematic initial side view of the metallomacrocycle **1** with the components highlighted by different colors, embedded in a fully hydrated POPC (1-Palmitoyl-2-oleoylphosphatidylcholine, palmitoyloleoylphosphatidylcholine) membrane. Parts of

water, ions and lipids were omitted for clarity, yet still illustrating membrane packing and water filling in the simulation box. (b) Initial construction with the macrocycle highlighted in red sitting in the center parallel to the surface of the membrane, depicted by the two wireframe surfaces at the level of the phosphate atoms (left). During equilibration, very rapidly, the macrocycle reorients to adopt a tilted orientation as shown in (right). (c) A cumulated view from the 20 ns trajectory, illustrating the peptide lateral arm flexibility in the membrane. (d) Water molecules inside the macrocycle environment.

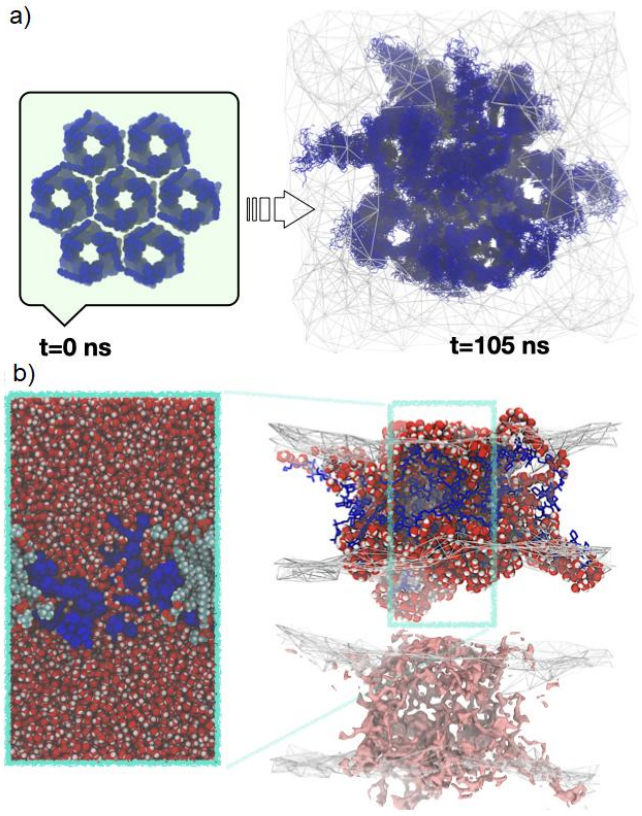

Figure 4. (a) Simulation of a 7-mer of compound **1** (in blue), starting from the arrangement shown at t=0 ns (looking from above the membrane down the membrane normal) toward a cumulative view from 85 to 105 ns to illustrate flexibility. (b) Different views of the water network (water in white and red, surface and hydrogen bonds in pink). The POPC membrane is shown by the connectivity of the phosphorus atoms of the individual leaflets (in white). Parts of water, ions and lipids have been omitted for clarity.

Molecular dynamic simulations. Three molecular dynamics simulations of compound **1** were performed in a fully hydrated membrane environment to probe its capacity to form artificial water channels and transport water across membranes. First, we examined how a single instance of compound **1** behaves in a membrane environment of pure POPC. For the simulation, the axis of the macrocycle was aligned with the membrane normal, which was then oriented along the Y-axis, perpendicular to the plane of the membrane coincident with the XZ-plane (Figure 3b left). The simulation shows the rapid reorientation of the macrocycle in the membrane (Figure 3b right).

In isolation, it is unstable when starting with its central ring horizontally aligned in the membrane. This leads to a general skew of the whole compound within the membrane due to ring tilting, which restricts the internal channel space. This observation was confirmed by two independent 20 ns simulations, which indicated variable flexibility of the compound. The central macrocycle remained fairly fixed in the tilted position, whereas the peptide-PEG sidechains exhibited considerable flexibility, with some PEG chains pending in water (Figure 3c). The experimental data showed that transport performances are concentration dependent, so the aggregation on the metallomacrocycle **1** might play a role using virtual reality,[29] we then built a larger assembly of 6 instances of **1** arranged in a hexagon around a central instance. This simulation was run for more than 100 ns, resulting in an irregular membrane-inserted aggregate producing sponge-like water passages (Figure 4).

Overall, all simulation results indicate that membrane-spanning hydration can be maintained and stabilized by the inserted metallomacrocycle **1**, although the conformation of the molecule is distorted by membrane pressure, aggregation, and out-of-plane orientation of the cycle (Figure S8). Figure 3d shows the hydration of the compound throughout the simulation. The water structure stabilizes with time, along the entire length of the membrane despite the unexpected asymmetric position and orientation of the compound within the membrane (SI Movie). We observed a few water passages through the channel core and many permeation events through the sponge-like water network ramifications at the interfaces between the instances of compound **1** and the lipid environment.

The orientation of the molecules reflects a porous structure and the initial transient appearance of water clusters inside the channel is in the region of the peptide lateral arms followed the water cluster stabilization in the central metallomacrocycle **1** pore interacting via Ni^{2+}salphen centers. The channel preference to form interconnected channel---H_2O---H_2O networks is the major factor determining their water / ion permselectivity. Contrary to carrier ions diffusion, proton translocation *via* directional H-bonds of water clusters is a structural diffusion and is strongly depending on the water cluster stabilization, which seems to be still very dynamic as observed in experimental proton translocation studies.[30]

The metallomacrocyclic **1** channel architecture is a very intriguing system. It is very tempting to equate that permeable water cluster sponge-like constructs are stabilized in the bilayer membrane. The assumption is that dynamic H-bonding with lateral peptide arms and hydrophobic interactions would initiate the water cluster formation, providing further premises for the stabilization of water cluster translocation pathways through the central metallo-macrocycle via Ni^{2+}-salphen centers in the center of the membrane. The water cluster stabilization confers to these channels self-protective behaviors against ions, as the cation/anion insertion will be energetically unfavorable, impeding the water cluster formation.

CONCLUSIONS

In conclusion, we have demonstrated here that self-assembled metallomacrocyclic-channels **1** can be obtained from salphen-peptide decorated ligands and Ni^{2+} metal ions present enhanced selective water permeability with almost total ion-rejection across a lipid bilayer. Slight tilted orientation of the macrocycle in the membrane and the very dynamic disposition of peptide lateral arms surrounding the macrocyclic cavity of the channels make them highly adaptive of transporting water at a rate one order of magnitude lower as for the natural AQP. These values are practically within the same order of magnitude $\sim 10^7$ water molecules/s/ channel as those observed for other pillararenes channels reported by Hou et al.[12,31] or by us[13] or hydroxy channels.[32,33] More importantly, salt rejection and the extremely low proton permeability through hydrophobically sterically restricted channels, offer the closest functional mimic of the natural AQP through a synthetic scaffold. These channels can be easily synthesized *via* simple self-assembly processes from simple components and are the first ones of this class of metallosupramolecular channels showing selective water permeation. Within this context, the metallomacrocyclic channels reported here may be considered as a novel important milestone on the way to the systematic discovery of synthetically accessible artificial water channels. They open up new directions and perspectives in AWCs research towards the construction of biomimetic membranes for desalination.[14]

ASSOCIATED CONTENT

Supporting Information

This material is available free of charge at the ACS Publications website.

Details about kinetic data of water permeabilities using D(+) sucrose and NaCl as Osmolytes. $M^+ = Na^+$, K^+, Rb^+ and Cs+ ion transport activities expressed as fluorescence intensities at different concentration of 1. Hill analysis results of complex 1 with FCCP. Initial and final snapshot of the molecular simulation after 20 ns.

AUTHOR INFORMATION

Corresponding Authors

Mihail Barboiu – *Institut Europeen des Membranes, Adaptive Supramolecular Nanosystems Group, University of Montpellier, ENSCM-CNRS, UMR5635, 34095 Montpellier, France;* https://orcid.org/0000-0003-0042-9483; Email: mihail-dumitru.barboiu@umontpellier.fr; Homepage: nsa-systems-chemistry.fr

Eiji Yashima – *Department of Molecular Design and Engineering, Graduate School of Engineering, Nagoya University Chikusa-ku, Nagoya 464-8603, Japan; Department of Molecular and Macromolecular Chemistry, Graduate School of Engineering, Nagoya University Chikusa-ku, Nagoya 464-8603, Japan;* E-mail: yashima@chembio.nagoya-u.ac.jp; Homepage: http://www.helix.chembio.nagoya-u.ac.jp/e/TOP.html

Authors

Li-Bo Huang – *School of Chemical Engineering and Technology, Hainan University, Haikou 570228, China; Institut Europeen des Membranes, Adaptive Supramolecular Nanosystems Group, University of Montpellier, ENSCM-CNRS, UMR5635, 34095 Montpellier, France*

Fumihiko Mamiya – *Department of Molecular Design and Engineering, Graduate School of Engineering, Nagoya University Chikusa-ku, Nagoya 464-8603, Japan*

Marc Baaden – *Laboratoire de Biochimie Théorique, CNRS, Université Paris Cité, 13 rue Pierre et Marie Curie, F-75005, Paris, France*

Notes

The authors declare no competing financial interest.

ACKNOWLEDGMENT

The authors wish to acknowledge the Agence Nationale de la Recherche for financial support (ANR-22-CE06-0024-02, BIOWATER)

REFERENCES

(1) Saier, Jr., M.H. Families of Proteins Forming Transmembrane Channels. *J. Membr. Biol.* **2000**, *175*, 165–180.

(2) King, L. S.; Kozono, D.; Agre, P. From Structure to Disease: The Evolving Tale of Aquaporin Biology. *Nat. Rev. Mol. Cell Biol.* **2004**, *5*, 687–698.

(3) Cukierman, S. Proton Mobilities in Water and in Different Stereoisomers of Covalently Linked Gramicidin A Channels. *Biophys. J.* **2000**, *78*, 1825–1834.

(4) Sisson, A. L.; Shah, M. R.; Bhosale, S.; Matile, S. Synthetic Ion Channels and Pores (2004–2005). *Chem. Soc. Rev.* **2006**, *35*, 1269–1286.

(5) Lehn, J.-M. in *Physical Chemistry of Transmembrane Ion Motions* (ed. G. Spach) Elsevier Amsterdam, **1983**, pp. 181–207.

(6) Gokel, G. W.; Murillo, O. Synthetic Organic Chemical Models for Transmembrane Channels. *Acc. Chem. Res.* **1996**, *29*, 425–432.

(7) Otis, F.; Racine-Berthiaume, C.; Voyer, N. How Far Can a Sodium Ion Travel within a Lipid Bilayer? *J. Am. Chem. Soc.* **2011**, *133*, 6481–6483.

(8) Jullien, L.; Lehn, J.-M. The "Chundle" Approach to Molecular Channels Synthesis of a Macrocycle-Based Molecular Bundle. *Tetrahedron Lett.* **1988**, *29*, 3803–3806.

(9) Hu, X. B.; Chen, Z.; Tang, G. Hou, J.-L.; Li, Z.-T. Single-Molecular Artificial Transmembrane Water Channels. *J. Am. Chem. Soc.* **2012**, *134*, 8384–8387.

(10) Chen, L.; Si, W.; Zhang, L.; Tang, G.; Li, Z.-T.; Hou, J.-L. Chiral Selective Transmembrane Transport of Amino Acids through Artificial Channels. *J. Am. Chem. Soc.* **2013**, *135*, 2152–2155.

(11) Si, W.; Li, Z.-T.; Hou, J.-L. Voltage-Driven Reversible Insertion into and Leaving from a Lipid Bilayer: Tuning Transmembrane Transport of Artificial Channels. *Angew. Chem. Int. Ed.* **2014**, *53*, 4578–4581.

(12) Yan, Z.-J.; Wang, D.; Ye Z.; Fan, T.; Wu, G.; Deng, L.; Yang, L.; Li, B.; Liu, J.; Ma, T.; Dong, C.; Li, Z.-T.; Xiao, L.; Wang, Y.; Wang, W.; Hou, J.-L. Artificial Aquaporin That Restores Wound Healing of Impaired Cells. *J. Am. Chem. Soc.* **2020**, *142*, 15638–15643.

(13) Strilets, D.; Fa, S.; Hardiagon, A.; Baaden M.; Ogoshi, T.; Barboiu, M. Biomimetic Approach for Highly Selective Artificial Water Channels Based on Tubular Pillar[5]arene Dimers. *Angew. Chem.* **2020**, *132*, 23413–23419; *Angew. Chem. Int. Ed.* **2020**, *59*, 23213–23219.

(14) Huang, L.-B.; Di Vincenzo, M.; Li, Y.; Barboiu, M. Artificial Water Channels: Towards Biomimetic Membranes for Desalination. *Chem. Eur. J.* **2021**, *27*, 2224–2239.

(15) Zheng, S.-P.; Huang, L.-B.; Sun, Z.; Barboiu, M. Self-Assembled Artificial Ion-Channels toward Natural Selection of Functions.

Angew. Chem. **2021**, *133*, 574–606; *Angew. Chem. Int. Ed.* **2021**, *60*, 566–597.
(16) Barboiu, M.; Le Duc, Y.; Gilles, A.; Cazade, P.-A.; Michau, M.; Legrand, Y.-M.; van der Lee, A.; Coasne, B.; Parvizi, P.; Post, J.; Fyles. T. An Artificial Primitive Mimic of The Gramicidin-A Channel. *Nat. Commun.* **2014**, *5*, 4142.
(17) (a) Le Duc, Y.; Michau, M.; Gilles, A.; Gence, V.; Legrand, Y.-M.; van der Lee, A.; Tingry, S.; Barboiu, M. Imidazole-Quartet Water and Proton Dipolar Channels. *Angew. Chem.* **2011**, *123*, 11568–11574; *Angew. Chem. Int. Ed.* **2011**, *50*, 11366–11372; (b) Licsandru, E.; Kocsis, I.; Shen, Y.-X.; Murail, S.; Legrand, Y.-M.; van der Lee, A.; Tsai, D.; Baaden, M.; Kumar, M.; Barboiu, M. Salt-Excluding Artificial Water Channels Exhibiting Enhanced Dipolar Water and Proton Translocation. *J. Am. Chem. Soc.* **2016**, *138*, 5403–5409.
(18) Fyles, T. M.; Tong, C. C. Predicting Speciation in The Multi-Component Equilibrium Self-Assembly of a Metallosupramolecular Complex. *New J. Chem.* **2007**, *31*, 655–661.
(19) Fujita, M.; Yazaki, J.; Ogura, K. Preparation of A Macrocyclic Polynuclear Complex, $[(en)Pd(4,4'\text{-}bpy)]_4(NO_3)_8$ (en = Ethylene Diamine, bpy = Bipyridine), Which Recognizes an Organic Molecule in Aqueous Media. *J. Am. Chem. Soc.* **1990**, *112*, 5645–5647.
(20) Jung, M.; Kim, H.; Baek, K.; Kim, K. Synthetic Ion Channel Based on Metal-Organic Polyhedra. *Angew. Chem.* **2008**, *120*, 5839–5841; *Angew. Chem. Int. Ed.* **2008**, *47*, 5755–5757.
(21) Kawano, R.; Horike, N.; Hijikata, Y.; Kondo, M.; Carné-Sánchez, A.; Larpent, P.; Ikemura, S.; Osaki, T.; Kamiya, K.; Kitagawa, S.; Takeuchi, S.; Furukawa, S. Metal-Organic Cuboctahedra for Synthetic Ion Channels with Multiple Conductance States. *Chem* **2017**, *2*, 393–403.
(22) Mahon, E.; Garai, S.; Müller, A.; Barboiu, M. Biomimetic Approach for Ion Channels Based on Surfactant Encapsulated Spherical Porous Metal-Oxide Capsules. *Adv. Mater.* **2015**, *27*, 5165–5170.
(23) Kulikov, O. V.; Li, R.; Gokel, G. W. A Synthetic Ion Channel Derived from a Metallogallarene Capsule That Functions in Phospholipid Bilayers. *Angew. Chem.* **2009**, *121*, 381–383; *Angew. Chem. Int. Ed.* **2009**, *48*, 375–377.
(24) Mamiya, F.; Ousaka, N.; Yashima, E. Remote Control of the Planar Chirality in Peptide-Bound Metallomacrocycles and Dynamic-to-Static Planar Chirality Control Triggered by Solvent-Induced 3(10)-to-α-Helix Transitions. *Angew. Chem.* **2015**, *127*, 14650–14654; *Angew. Chem. Int. Ed.* **2015**, *54*, 14442–14446.
(25) Hjørringgaard, C. U.; Vad, B. S.; Matchkov, V. V.; Nielsen, S. B.; Vosegaard, T.; Nielsen, N. C.; Otzen, D. E.; Skrydstrup, T. Cyclodextrin-Scaffolded Alamethicin with Remarkably Efficient Membrane Permeabilizing Properties and Membrane Current Conductance. *J. Phys. Chem. B* **2012**, *116*, 7652–7659.
(26) Di Vincenzo, M.; Tiraferri, A.; Musteata, V.-E.; Chisca, S.; Sougrat, R.; Huang, L.-B.; Nunes, S. P.; Barboiu, M. Biomimetic Artificial Water Channel Membranes for Enhanced Desalination. *Nat. Nanotechnol.* **2021**, *16*, 190–196.
(27) Matile, S.; Sakai, N. in *Analytical Methods in Supramolecular Chemistry*, Schalley, C. A., Ed. Wiley-VCH: Weinheim, pp 381–418, **2007**.
(28) Li, Y.-H.; Zheng, S.-P.; Legrand, Y.-M.; Gilles, A.; Van der Lee, A.; Barboiu, M. Structure-Driven Selection of Adaptive Transmembrane Na^+ Carriers or K^+ Channels. *Angew. Chem.* **2018**, *130*, 10680–10684; *Angew. Chem. Int. Ed.* **2018**, *57*, 10520–10524.
(29) Baaden, M. *Virtual Reality@Intelligent Hardware*. **2022**, 4, 324–341
(30) Decoursey, T. E. Voltage-Gated Proton Channels and Other Proton Transfer Pathways. *Physiol. Rev.* **2003**, *83*, 475–579.
(31) Xiao, Q.; Fan, T.; Wang, Y.; Li, Z.-T.; Hou, J. L.; Wang, Y. Artificial Water Channel that Couples with Cell Protrusion Formation. *CCS Chem.* **2023**, 1-8.
(32) Huang, L.-B.; Hardiagon, A.; Kocsis, I.; Jegu, C.-A.; Deleanu, M.; Gilles, A.; van der Lee, A.; Sterpone, F.; Baaden, M.; Barboiu, M. Hydroxy Channels–Adaptive Pathways for Selective Water Cluster Permeation. *J. Am. Chem. Soc.* **2021**, *143*, 4224–4233.
(33) Mondal, D.; Dandekar, B. R.; Ahmad, M.; Mondal, A.; Mondal J.; Talukdar P. Selective and rapid water transportation across a self-assembled peptide-diol channel via the formation of a dual water array. *Chem. Sci.*, **2022**, *13*, 9614–9623.

Table of Content